

# UC Berkeley

## UC Berkeley Previously Published Works

### Title

Chemically recyclable thermoplastics from reversible-deactivation polymerization of cyclic acetals

### Permalink

<https://escholarship.org/uc/item/33t3x0rw>

### Journal

Science, 373(6556)

### ISSN

0036-8075

### Authors

Abel, Brooks A  
Snyder, Rachel L  
Coates, Geoffrey W

### Publication Date

2021-08-13

### DOI

10.1126/science.abh0626

Peer reviewed

## POLYMER CHEMISTRY

## Chemically recyclable thermoplastics from reversible-deactivation polymerization of cyclic acetals

Brooks A. Abel<sup>1</sup>†, Rachel L. Snyder<sup>1</sup>†, Geoffrey W. Coates<sup>1\*</sup>

Identifying plastics capable of chemical recycling to monomer (CRM) is the foremost challenge in creating a sustainable circular plastic economy. Polyacetals are promising candidates for CRM but lack useful tensile strengths owing to the low molecular weights produced using current uncontrolled cationic ring-opening polymerization (CROP) methods. Here, we present reversible-deactivation CROP of cyclic acetals using a commercial halomethyl ether initiator and an indium(III) bromide catalyst. Using this method, we synthesize poly(1,3-dioxolane) (PDXL), which demonstrates tensile strength comparable to some commodity polyolefins. Depolymerization of PDXL using strong acid catalysts returns monomer in near-quantitative yield and even proceeds from a commodity plastic waste mixture. Our efficient polymerization method affords a tough thermoplastic that can undergo selective depolymerization to monomer.

Plastics are among the most high-performance and cost-effective materials available today. Consumer industries depend on the versatile properties of plastics. As a result, plastic production increases by ~8% annually, with single-use packaging materials making up nearly 40% of plastic products (1, 2). However, the mass manufacture and uncontrolled disposal of plastics has come at both economic and environmental costs (1, 3–7). Currently, most collected postconsumer plastics are processed for reuse via downcycling approaches such as mechanical recycling, affording relatively small quantities of low-value materials with diminished properties (2, 8, 9). As the plastics crisis grows, global organizations and governments (10, 11) are targeting more promising strategies to simultaneously combat the environmental and economic impacts of the plastics problem. These methods include up-cycling, where plastic waste is used as a feedstock for value-added materials (12–16) and chemical recycling to monomer (CRM). CRM converts plastic waste directly back to monomer, enabling a circular plastics economy that both mitigates the need for continuous feedstock sourcing and could potentially eliminate the accumulation of plastic waste. To reduce our dependence on fossil fuels, prevent the accumulation of millions of tons of plastic waste each year, and turn massive economic losses into gains, the development of a circular plastics economy via CRM must be at the forefront of sustainability efforts (17, 18).

Polymers derived from moderately strained heterocyclic monomers are viable candidates

for CRM because of their moderate ceiling temperatures ( $T_c < 250^\circ\text{C}$ ), the temperature at which the change in Gibbs free energy ( $\Delta G = 0$  for polymerizations where both the change in enthalpy ( $\Delta H$ ) and the change in entropy ( $\Delta S$ ) are negative (19). To date, polyesters (20–25), polycarbonates (26–29), and polymers derived from other heterocyclic monomers (30–35) are capable of CRM. Several of these systems exhibit noteworthy properties. Chen and co-workers reported on the synthesis of poly[*trans*-hexahydro-2(3*H*)-benzofuranone], which displayed high tensile stress at break ( $\sigma_B = 55$  MPa), high melting temperature ( $T_m$ ) values ( $\geq 126^\circ\text{C}$ ), and good thermal stability [decomposition temperature ( $T_d$ ) =  $340^\circ\text{C}$ ] (23). Helms and co-workers synthesized cross-linked polymers comprising diketoenamine linkages, which were depolymerized in the presence of mixed plastic waste (33). Mecking and co-workers developed long-chain aliphatic polyesters with polyolefin-like mechanical properties that were synthesized on a large scale from biorenewable monomers and chemically recycled via solvolysis (36). Moving forward, important advancements to these foundational reports (and others) will include implementing easily accessible monomers, improving the efficiency of polymer syntheses, accessing useful material properties, and invoking simple processes for depolymerization to monomer (9, 12, 37). Designing systems that meet these criteria will enable the widespread use of chemically recyclable polymers.

Polyacetals are promising candidates for CRM because their dynamic acetal functionalities facilitate depolymerization at relatively low temperatures ( $<150^\circ\text{C}$ ) (34). They also possess suitable thermal and chemical stability for real-world application, as evidenced by the commercialization of polyoxymethylene (POM) as an engineering thermoplastic (38). Polyacetals are commonly synthesized from cyclic

acetal monomers, which are readily made on a large scale from diols and formaldehyde (39).

1,3-Dioxolane (DXL) is commercially synthesized in a single step on a large scale from common industrial C1 and C2 feedstocks—formaldehyde and ethylene glycol, respectively—both of which also have bioderived routes (34, 40). Early work on poly(1,3-dioxolane) (PDXL) suggested its potential applications (Fig. 1A) (41). However, consistently obtaining high molecular weight polyacetals has remained challenging because cyclic acetal polymerization using Brønsted or Lewis acid catalysts affords poor molecular weight control (Fig. 1B) (42). Therefore, we sought to achieve molecular weight control during the cationic ring-opening polymerization (CROP) of DXL.

In typical living and/or controlled cationic polymerizations, dormant halide-terminated chain ends generated from discrete initiators are reversibly activated by a Lewis acid catalyst. This reversible-deactivation mechanism maintains low cation concentrations, a requirement for minimizing undesired termination and irreversible chain transfer. Living cationic polymerizations were initially developed in the 1970s by Higashimura, Sawamoto, and colleagues to polymerize vinyl ether and *N*-vinylcarbazole monomers (43, 44) and later were adapted to isobutylene systems by Faust and Kennedy (45). More recently, Aoshima and co-workers used a reversible-deactivation strategy to copolymerize vinyl ethers and cyclic acetals (46). In this work, we identify an initiator and Lewis acid catalyst system capable of promoting reversible deactivation of halide-terminated polyacetals to achieve both molecular weight control and high living chain-end retention (Fig. 1C) (47).

In reversible-deactivation CROP (RD-CROP), the active  $3^\circ$  oxonium and oxocarbenium species present during CROP of cyclic acetals are in equilibrium with dormant halomethyl ether species (Fig. 2A). Therefore, we selected chloromethyl methyl ether (MOMCl) as the initiator for RD-CROP to mirror the dormant halide-terminated polyacetal chain ends. To prevent undesired initiation or chain transfer by protic impurities, the sterically hindered base 2,6-di-*tert*-butyl pyridine (DTBP) was used as a proton trap (48). We screened a range of commercial Lewis acid catalysts of the form  $\text{MCl}_n$  [ $\text{M} = \text{B(III)}, \text{Al(III)}, \text{Ga(III)}, \text{In(III)}, \text{Sb(III)}/\text{Sb(V)}, \text{Bi(III)}, \text{Sn(IV)}, \text{Zn(II)}, \text{Fe(III)}, \text{Ti(IV)}, \text{Zr(IV)}, \text{or Hf(IV)}$ ] owing to their prior use in cationic polymerizations and Friedel-Crafts reactions. In the presence of a Lewis acid and halomethyl ether, cyclic acetal polymerization can proceed via three pathways: (i) initiation by Brønsted acid impurities, (ii) monomer activation with the Lewis acid catalyst, or (iii) ionization of halomethyl ether chain ends by the Lewis acid catalyst (i.e., RD-CROP). We determined the selectivity

<sup>1</sup>Department of Chemistry and Chemical Biology and Joint Center for Energy Storage Research, Baker Laboratory, Cornell University, Ithaca, NY 14853, USA.

\*Corresponding author. Email: coates@cornell.edu

†These authors contributed equally to this work.

of each catalyst toward RD-CROP of DXL using  $MCl_n$  only (method A),  $MCl_n + DTBP$  (proton trap; method B), or  $MCl_n + DTBP + MOMCl$  initiator (method C). Catalysts were deemed viable for RD-CROP if polymerization did not occur using method B (i.e., both  $H^+$  activation and Lewis acid monomer activation were absent) but proceeded when initiator was added to the system (method C; fig. S1). No polymerization was observed within 18 hours when the Lewis acids  $BCl_3$ ,  $AlCl_3$ ,  $SbCl_3$ ,  $BiCl_3$ ,  $TiCl_4$ ,  $ZrCl_4$ , or  $HfCl_4$  were used in the presence or absence of MOMCl (table S2). Polymerization occurred in both the presence and absence of MOMCl when the Lewis acids  $GaCl_3$ ,  $SbCl_5$ ,  $SnCl_4$ , or  $FeCl_3$  were used (table S2), indicating that these Lewis acids directly activate monomer.  $InCl_3$  and  $ZnCl_2$  catalyzed the polymerization of DXL exclusively in the presence of MOMCl. We hypothesize that the increased halophilicity of soft Lewis acids such as  $InCl_3$  and  $ZnCl_2$  improves selectivity toward chain-end activation relative to binding oxygens in the monomer or polymer (49).  $ZnCl_2$  demonstrated incomplete conversion, even at higher catalyst loadings over 18 hours. Meanwhile,  $InCl_3$  reached maximum conversion (~85%, based on measured standard state  $\Delta H^\circ$  and  $\Delta S^\circ$  values when  $[DXL]_0 = 8 M$ ; see below) in under 18 hours at lower catalyst loading and was selected for further optimization (table S2). Despite lower activity than In-based catalysts, Zn-based catalysts could be a more cost-effective alternative (23).

To increase the polymerization rate, we exchanged Cl with more-labile Br leaving groups to increase the extent of chain-end ionization (i.e., concentration of active chain ends). The  $InX_3/MOMX$  halide composition was varied from a [Br]:[Cl] ratio of 0:4 to 4:0 by combining the appropriate amounts of MOMCl, MOMBr,  $InCl_3$ , and  $InBr_3$  to achieve a particular halogen stoichiometry. At [Br]:[Cl] = 0:4, polymerization reached 81% conversion in 40 min. When [Br]:[Cl] was increased to 4:0, 81% conversion was reached in just 90 s, demonstrating a more than 25-fold increase in polymerization rate (Fig. 2B and table S3). In all cases, we observed a linear dependence of number-average molecular weight as measured by gel permeation chromatography ( $M_{n,GPC}$ ) on DXL conversion, suggesting living chain-end retention throughout the polymerization (table S3 and fig. S2).

RD-CROP with  $InBr_3/MOMBr$  showed excellent molecular weight control for DXL and other monocyclic acetal derivatives including 1,3-dioxepane (DXP), 1,3-dioxocane (DXC), 1,3,7-trioxocane (TXC), and the bicyclic acetal *trans*-hexahydro-1,3-benzodioxole (HBD) (Fig. 2C; figs. S3 to S7; and table S5). For each monomer derivative,  $M_{n,GPC}$  increases linearly with increasing monomer-to-initiator ratio

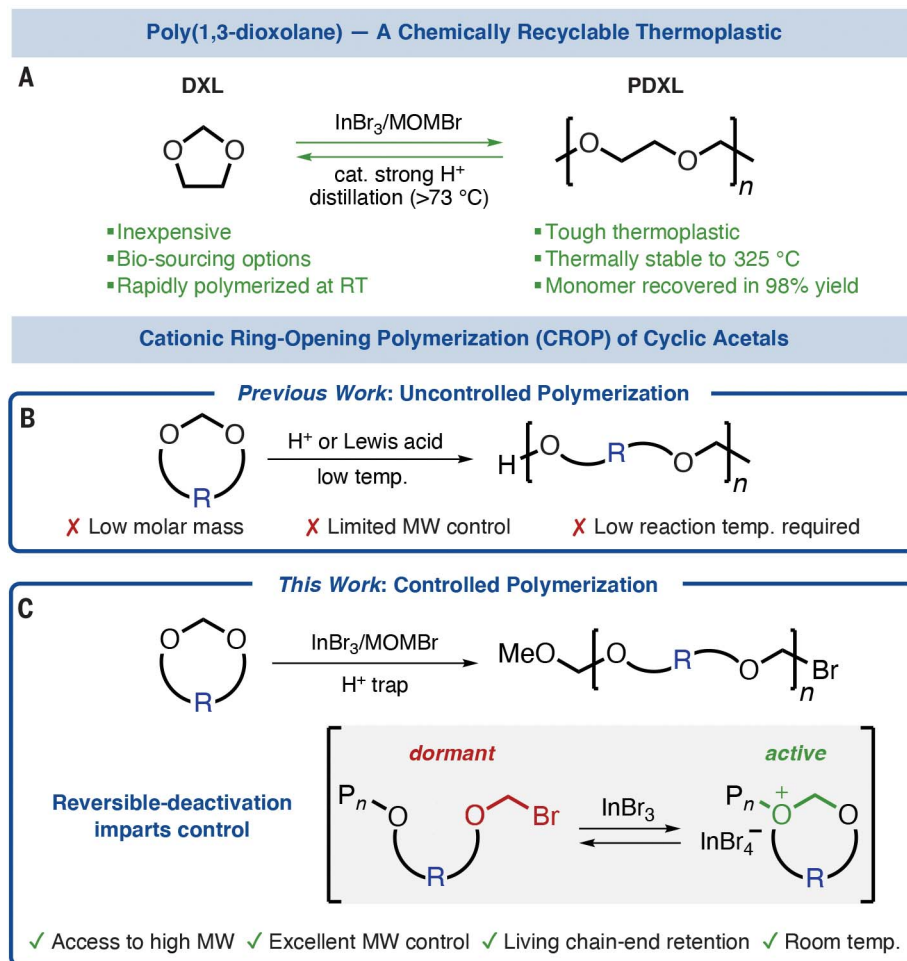


**Fig. 1. Methods of polyacetal synthesis.** (A) Polymerization of DXL is reversible through heating in acid. RT, room temperature. (B) Uncontrolled CROP of cyclic acetals using Brønsted or Lewis acid initiators affords poor molecular weight (MW) control. (C) RD-CROP imparts control over cyclic acetal polymerization. R, organic linker; MeO, methoxy group.

([monomer]<sub>0</sub>: [MOMBr]<sub>0</sub>), indicating that initiation by MOMBr is predominant. Sequential monomer additions over 24 hours during RD-CROP of DXL further confirmed living chain-end retention at room temperature (Fig. 2D).  $M_{n,GPC}$  values increased in proportion to the amount of DXL added, and no change in dispersity ( $\mathcal{D}$ ) was observed during the course of the experiment (table S6 and fig. S9).

Despite excellent molecular weight control, we consistently observed  $\mathcal{D}$  values ranging from 1.51 to 1.74 owing to transacetalization, a known phenomenon in CROP of cyclic acetals (50). During transacetalization, acetal linkages in the polymer backbone react with cationic polymer chain ends because of the similar nucleophilicities of cyclic and acyclic acetals (fig. S10). We confirmed transacetalization during RD-CROP of cyclic acetals by introducing increasing amounts of an acyclic acetal, diethoxymethane (DEM), relative to [MOMBr]

at a constant monomer-to-initiator ratio. Gel permeation chromatography (GPC) analyses show good agreement between theoretical molecular weights ( $M_{n,th}$ ) calculated using equation S2 (see supplementary materials) and experimental  $M_{n,GPC}$  values (table S7 and fig. S11). For all studied polyacetals, end-group analysis of low molecular weight samples was performed using matrix-assisted laser desorption/ionization–time-of-flight (MALDI-TOF) mass spectrometry. As anticipated, degenerative chain transfer to polymer via transacetalization gives a statistical 1:2:1 distribution of chain ends from the MOMBr initiator and sodium benzyloxide (NaOBn) quenching agent (figs. S10 to S14).

In previous reports, residual catalyst or acid species from incomplete polymer purification prematurely catalyzed depolymerization of polyacetals owing to the thermodynamics of polymerization and depolymerization (Fig. 2E;

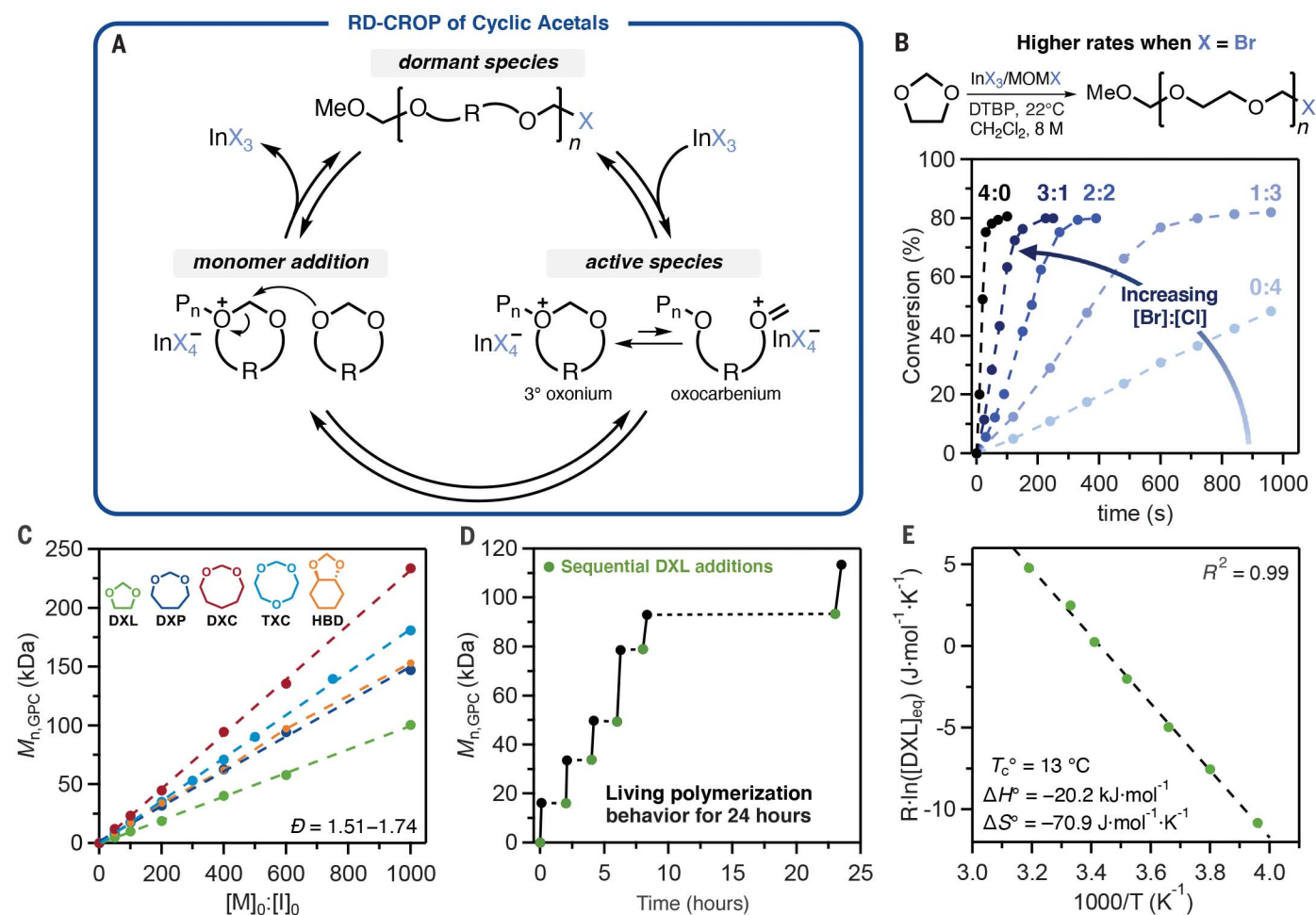


**Fig. 2. Reversible-deactivation cationic ring-opening polymerization of cyclic acetals.** (A) The proposed mechanism of cyclic acetal RD-CROP involves reversible chain-end activation by the  $InBr_3$  catalyst after MOMBr initiation. (B) Reaction rate increases with  $InX_3/MOMX$   $[Br]:[Cl]$  ratio in the RD-CROP

system. (C) Molecular weight control is observed with linear dependence of  $M_{n,GPC}$  on  $[monomer]_0:[MOMBr]_0$  for monomer scope. (D) High living chain-end retention is observed during RD-CROP of DXL. (E) Van't Hoff analysis of variable temperature NMR data provides  $\Delta H^\circ$ ,  $\Delta S^\circ$ , and  $T_c^\circ$  values for PDXL.

see below) (51). With an improved purification method (see supplementary materials), all five polyacetal derivatives exhibited excellent thermal stability by thermogravimetric analysis (TGA), with degradation temperatures at 5% mass loss ( $T_{d,5\%}$ ) above  $337^\circ C$  (fig. S17 and table S8). Isothermal TGA data shows >99% mass remaining after 2 hours at  $140^\circ C$  for each polyacetal derivative (fig. S18 and table S9).

Differential scanning calorimetry (DSC) was used to measure the thermal transition temperatures for each polyacetal derivative, some of which are semicrystalline (fig. S19 and table S10). Semicrystalline PDXL exhibits a low glass transition temperature ( $T_g$ ) of  $-63^\circ C$  and a  $T_m$  of  $58^\circ C$ . The  $T_m$  of PDXL is comparable to thermal transitions in several commercial materials, including poly(lactic acid) ( $T_g = 60^\circ C$ ), poly(ethylene terephthalate) ( $T_g = 61^\circ C$ ), poly( $\epsilon$ -caprolactone) ( $T_m = 60^\circ C$ ), and poly(ethylene oxide) ( $T_m = 66^\circ C$ ) (52). Both

thermal transitions in PDXL are invariant with molecular weight from 37.9 to 220 kDa (fig. S20 and table S11).

In general, tensile strength increases with polymer molecular weight. To date, the tensile properties of PDXL have been overlooked because prior catalyst systems typically yielded low molecular weight materials (see above) (42). To measure the effect of molecular weight on tensile properties, we synthesized PDXL on a 10-g scale with  $M_{n,GPC}$  values ranging from 37.9 to 220 kDa (fig. S21 and table S12). Bulk PDXL was melt pressed to give colorless, opaque films (Fig. 3A). Uniaxial tensile elongation tests were performed on the PDXL samples of increasing molecular weight to identify the critical molecular weight, above which robust properties are obtained (figs. S20 to S22 and tables S13 to S19). Low molecular weight PDXL (37.9 kDa), which is comparable to the highest previously reported molecular

weight (42), demonstrates poor mechanical properties, with a  $\sigma_B$  of only  $13.5 \pm 1.3$  MPa at  $5 \pm 0.3\%$  strain ( $\epsilon_B$ ) (table S14 and fig. S24). At 82.3 kDa, PDXL tensile properties increase significantly to  $\sigma_B = 33.3 \pm 1.2$  MPa and  $\epsilon_B = 640 \pm 45\%$  (table S16 and fig. S24). At 180 kDa, PDXL showed high tensile strength, with  $\sigma_B = 40.4 \pm 1.2$  MPa and  $\epsilon_B = 720 \pm 20\%$ , revealing the impressive toughness and ductility of PDXL at high molecular weights (Fig. 3A and table S19). In fact, the tensile strength of PDXL is comparable to the two most prevalent commodity plastic materials, isotactic polypropylene ( $\sigma_B = 26$  MPa and  $\epsilon_B = 420\%$ ) and high-density polyethylene ( $\sigma_B = 30.2$  MPa and  $\epsilon_B = 900\%$ ). Like other semicrystalline polymers, PDXL undergoes considerable strain-induced crystallization, forming visible white striations that give way to fibrous filaments after fracture (fig. S25).

The stability of the films at elevated temperature and/or humidity was studied by



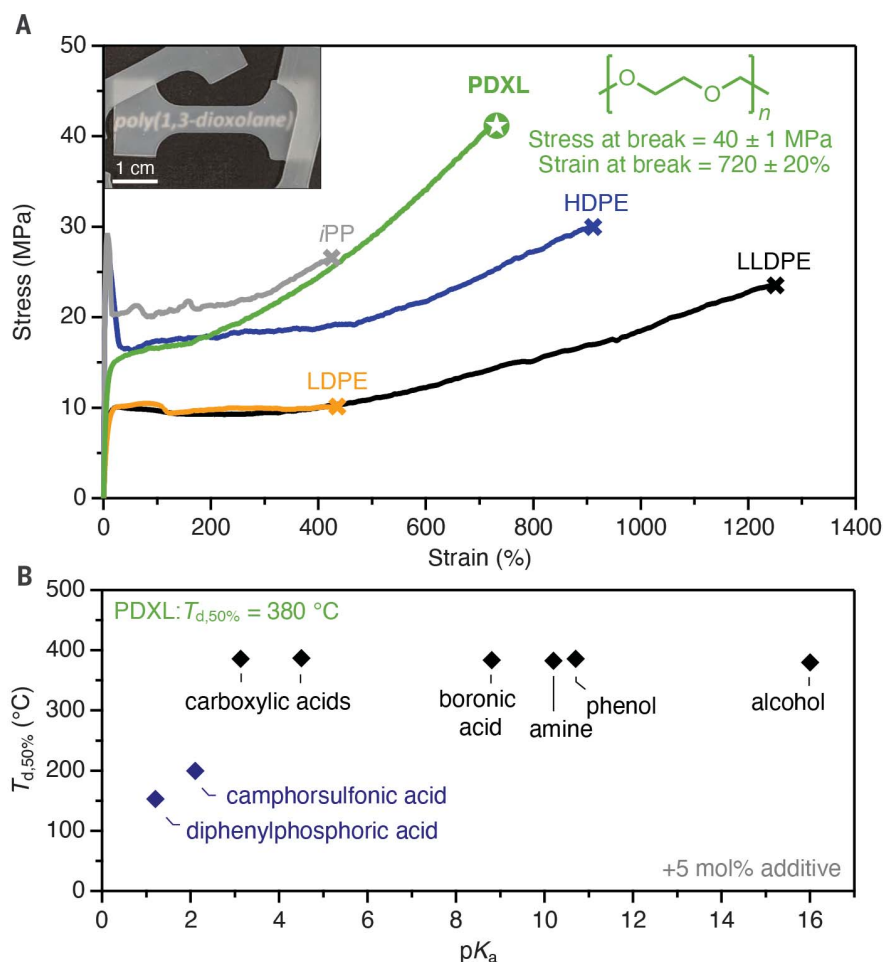


**Fig. 3. Tensile properties and thermal stability of poly(1,3-dioxolane).**

(A) PDXL exhibits high tensile strength comparable to isotactic polypropylene (iPP) and high-density polyethylene (HDPE). LDPE, low-density polyethylene; LLDPE, linear low-density polyethylene. Inset: Image of colorless, semicrystalline

PDXL films synthesized on multigram scales. (B) PDXL shows good thermal stability ( $T_{d,50\%} \geq 380^{\circ}\text{C}$ ) in the presence of weak acids and amines but degrades readily with strong acid additives ( $\text{pK}_a \leq 2.1$ ). (C) PDXL prototype items were formed by melt processing of PDXL films.

placing a PDXL sample (110 kDa, 100 mg) in a 20-ml vial under either a dry atmosphere or at 100% relative humidity. After 7 days at  $57^{\circ}\text{C}$ , the polymer samples exposed to dry or humid environments showed identical proton nuclear magnetic resonance ( $^1\text{H}$  NMR) spectra to those of the pristine material and no decrease in  $M_n$ . These experiments highlight the stability of PDXL at elevated temperatures for prolonged periods of time, even at 100% relative humidity (fig. S26). Additionally, no transesterification was observed after polymer isolation, confirming full removal of active catalytic species from the polymer samples during purification (fig. S27). High molecular weight PDXL (180 kDa) is readily soluble in  $\text{CH}_2\text{Cl}_2$  but demonstrates good solvent resistance and minimal swelling toward hexanes, acetone, methyl ethyl ketone (MEK), and ethanol (EtOH) with <3% dissolution by mass after 100 days submerged in these solvents under ambient conditions (fig. S28 and table S20). PDXL showed some solubility in

tetrahydrofuran, with 90 wt % remaining after 100 days. Submersion in water for extended periods of time results in partial dissolution, reaching 17% mass loss in 7 days and 64% mass loss over 100 days. Both high (182 kDa) and low (37.9 kDa) molecular weight PDXL showed identical GPC traces after 100 days in  $\text{H}_2\text{O}$ , indicating that PDXL is resistant to hydrolysis under neutral pH conditions over time. Although the hydrophilicity of PDXL precludes its use in some applications, many plastic products, such as air pillows, protective pouches, or molded packaging, require robust tensile strengths but remain dry during use (Fig. 3C). Detailed  $^1\text{H}$  NMR analysis of PDXL in  $\text{CDCl}_3$  or  $\text{D}_2\text{O}$  at  $50^{\circ}\text{C}$  for 48 hours showed no change in the NMR spectra, such as the appearance of any degradation by-products including formaldehyde, epoxides, alcohols, or monomer (fig. S29). Therefore, although PDXL dissolves in water, it does not hydrolytically degrade, even above the ceiling temperature, in the absence of an acid catalyst.

### C Protective Pouches



### Molded Packaging



### Air Pillows



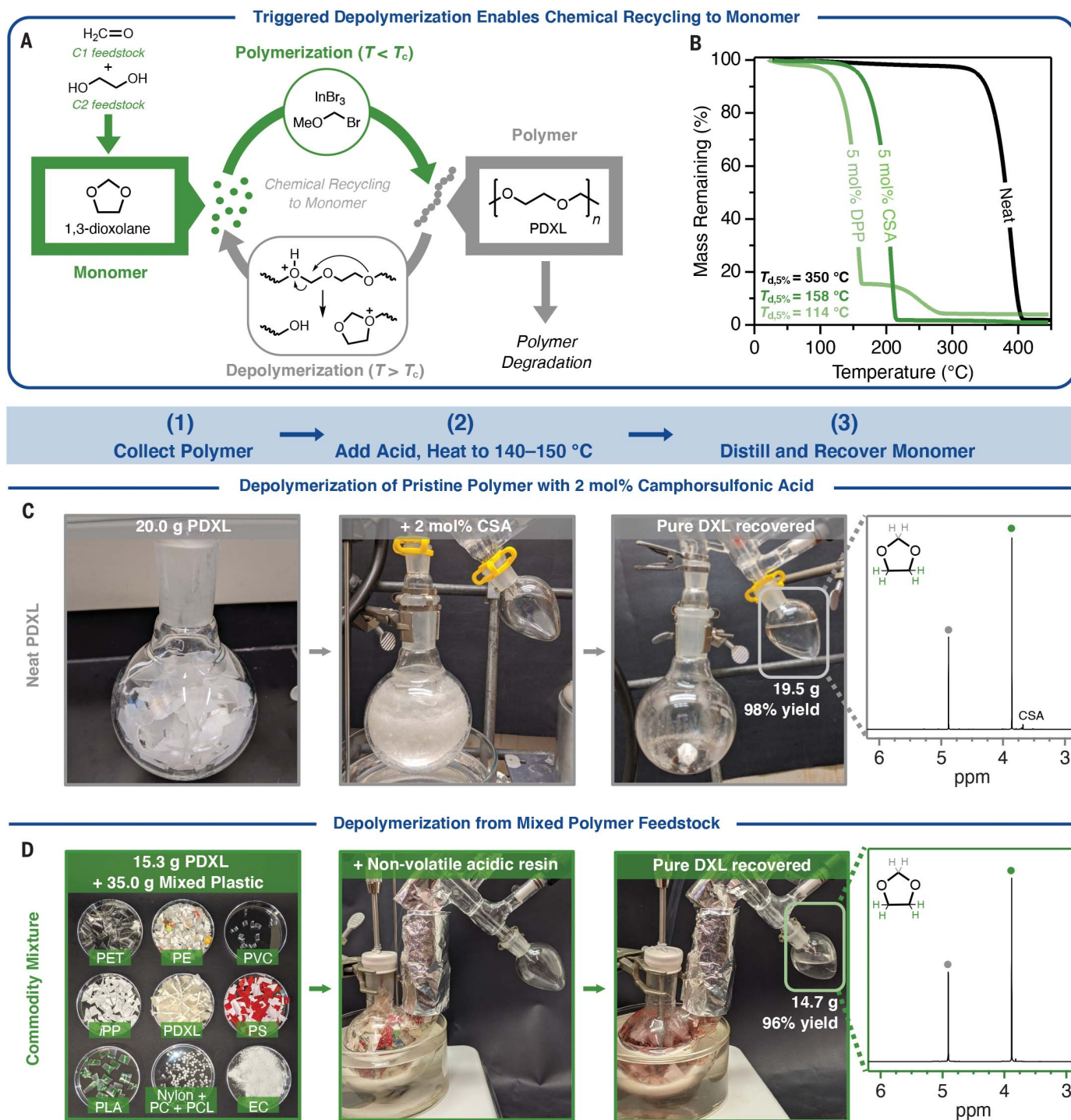


**Fig. 4. Chemical recycling to monomer of poly(1,3-dioxolane).** (A) DXL can be polymerized to PDXL and chemically recycled to monomer. (B) PDXL is thermally stable to  $T_{d,5\%} = 353^\circ\text{C}$  but readily depolymerized with 5 mol % added CSA or DPP. (C) PDXL was depolymerized via distillation in ambient atmosphere at  $150^\circ \pm 5^\circ\text{C}$  over 60 min to recover DXL monomer in near-quantitative yields.  $^1\text{H}$  NMR of the recovered monomer shows only DXL and trace amounts of CSA (ppm, parts per

million), which is readily removed during monomer drying with  $\text{CaH}_2$ . (D) Using a polymer-supported acid catalyst, CRM of PDXL from a mixed commodity plastics feedstock yields exclusively DXL monomer without contamination by dyes, plasticizers, or other additives. PET, polyethylene terephthalate; PE, polyethylene; PVC, polyvinyl chloride; PS, polystyrene; PLA, polylactic acid; PC, polycarbonate; PCL, poly( $\epsilon$ -caprolactone); EC, ethyl cellulose.



( $DXL_{eq}$ ) was measured as a function of temperature (fig. S31 and table S21) (30). The resultant van't Hoff plot and equations S5 to S7 (see supplementary materials) were used to determine the standard state  $\Delta H^\circ$ ,  $\Delta S^\circ$ , and  $T_c^\circ$  values for RD-CROP of DXL (Fig. 2E and fig. S32). PDXL demonstrates  $\Delta H^\circ = -20 \text{ kJ}\cdot\text{mol}^{-1}$ ,  $\Delta S^\circ = -70.9 \text{ J}\cdot\text{mol}^{-1}\cdot\text{K}^{-1}$ , and a relatively low  $T_c^\circ$  of  $13^\circ\text{C}$ , which is in good agreement with previously reported values (table S22) (53).

Given its low  $T_c$ , it is essential that PDXL undergoes depolymerization only in the presence of an external catalyst to avoid unintended degradation during use. Methylene acetals are known to remain stable toward weak acids and bases (54). Similarly, PDXL showed excellent thermal stability in the presence of acid or base additives across a range of  $pK_a$  values (where  $K_a$  is the acid dissociation constant) (Fig. 3B). Additives with relatively low volatility were chosen to provide the largest temperature window possible before boiling or sublimation of the additive occurred. Polymer thermal stability was quantified using the degradation temperature at 50% mass remaining ( $T_{d,50\%}$ ) to account for mass loss from the additive (8 to 15 wt %) (table S23). PDXL retains  $T_{d,50\%}$  values near  $380^\circ\text{C}$  with 5 mol % loading of weaker acids, including citric acid ( $pK_{a,1} = 2.9$ ), *trans*-cinnamic acid ( $pK_a = 4.5$ ), or 4-tolylboronic acid ( $pK_a = 8.8$ ) (fig. S33 and table S23). Likewise, 5 mol % loadings of representative alcohols 4-*tert*-butyl phenol and 1-pentadecanol and nitrogen-containing bases octylamine, tributylamine, and 7-methyl-1,5,7-triazabicyclo[4.4.0]decene (MeTBD) did not affect PDXL degradation (figs. S34 and S35 and table S23). As expected, strong acids such as diphenylphosphoric acid (DPP;  $pK_a = 1.2$ ) and camphorsulfonic acid (CSA;  $pK_a = 2.1$ ) efficiently catalyzed PDXL degradation, affording accessible  $T_{d,50\%}$  values of  $153^\circ$  and  $200^\circ\text{C}$ , respectively (Fig. 4B and table S23). Lewis acidic lithium bis(trifluoromethane)sulfonimide and transition metal titanium(IV) isopropoxide also catalyzed PDXL degradation ( $T_{d,50\%}$  values of  $323^\circ$  and  $313^\circ\text{C}$ , respectively), although much less efficiently than did CSA and DPP (fig. S36 and table S23).

CSA was selected as a representative depolymerization catalyst as it is inexpensive and derived from biosourced material. The rate of acid-catalyzed degradation decreased slightly with increasing  $M_{n,GPC}$ . At 2 mol % CSA loading, the time to 25% mass loss at  $120^\circ\text{C}$  increased from 6.7 to 9.0 to 10.5 min for 27.9, 110, and 220 kDa PDXL in the melt, respectively (fig. S37 and table S24). As expected, increasing degradation rates were also observed at increasing temperatures ( $100^\circ$  to  $140^\circ\text{C}$ ) for a 127 kDa PDXL sample with 2 mol % added CSA (fig. S37). The rate of degradation (percent mass loss per second) was calculated from the initial slope of the isothermal TGA

experiments (90 to 70% mass remaining) and used to determine an Arrhenius activation energy of  $85.0 \text{ kJ/mol}$  [coefficient of determination ( $R^2$ ) = 0.998] for CSA-catalyzed PDXL depolymerization (fig. S38). Upon increasing the CSA loading from 5 to 10 to 15 mol %, the  $T_{d,5\%}$  of PDXL (182 kDa) decreased from  $157^\circ$  to  $108^\circ$  to  $80^\circ\text{C}$ , respectively. At 20 or 25 mol % added CSA, PDXL  $T_{d,5\%}$  values plateaued at  $73^\circ$  and  $74^\circ\text{C}$ , respectively, coinciding with the boiling point of DXL monomer (fig. S39 and table S25).

Once depolymerization is kinetically activated by the catalyst, the combined low  $T_c^\circ$  of PDXL and low volatility of DXL permit facile monomer collection via simple distillation at moderate temperatures under ambient pressure, an accessible and inexpensive procedure that could mitigate the need to transport substantial amounts of waste to specialized recycling facilities (16). We first doped PDXL (20.0 g; 60 to 220 kDa) with 2 mol % CSA. The catalyst was solvent-cast into the material in  $\text{CH}_2\text{Cl}_2$  to ensure a homogeneous dispersion of CSA and study the efficacy of PDXL CRM (Fig. 4C). A short-path distillation was then set up under ambient atmosphere, and the PDXL/CSA mixture was lowered into an oil bath preheated to  $140^\circ\text{C}$ . After heating for 14 min, pure DXL began collecting in the receiving flask. The distillation continued for 78 min in total, at which point only black residue from degraded CSA remained, and 19.5 g (98% yield) of pure DXL monomer was collected with trace amounts of CSA impurities, as confirmed by  $^1\text{H}$  NMR spectroscopy (fig. S40 and table S26). The recovered DXL was later dried over  $\text{CaH}_2$  and repolymerized using  $\text{InBr}_3/\text{MOMBr}$ -catalyzed RD-CROP in  $\text{CH}_2\text{Cl}_2$  at room temperature to give PDXL ( $M_{n,GPC} = 84.4 \text{ kDa}$ ) with identical tensile properties to pristine 80.7 kDa material (fig. S41 and table S27).

Plastics collected from mixed waste streams generally include a variety of dyes and/or pigments, plasticizers, stabilizers, and other impurities (9). A key advantage of CRM is the ability to isolate pure monomer from such complex mixtures, avoiding the need for time- and cost-intensive separation processes. To investigate the efficacy of selective PDXL depolymerization and DXL collection from a mixture of plastic waste, we performed CRM of PDXL in the presence of poly(ethylene terephthalate), high-density and low-density polyethylene, poly(vinyl chloride), isotactic polypropylene, polystyrene, poly(lactic acid), poly( $\epsilon$ -caprolactone), polycarbonate, nylon-6,6, ethyl cellulose, and the plasticizer bis(2-ethylhexyl) phthalate. The plastics used were either postconsumer materials containing dyes, additives, and plasticizers or were purchased from chemical suppliers (table S28). PDXL (15.3 g; 80 to 180 kDa) was then added to the mixture, and an acidic resin (Dowex-50, 5 wt %)

was selected as a nonvolatile catalyst (Fig. 4D). The heterogeneous mixture was then mechanically stirred at  $150^\circ \pm 5^\circ\text{C}$  under ambient atmosphere. A primary fraction of DXL monomer (13.8 g) was collected during the first 30 min. A second fraction (0.931 g) was collected over an additional 30 min, giving a total DXL yield of 96%. Most notably, the two collected fractions contained >99% DXL monomer in the presence of commodity plastics containing acid- and/or heat-sensitive linkages (i.e., esters, amides, carbonates, and glycosidic bonds) and small-molecule dyes and plasticizers (figs. S42 and S43). This result demonstrates that polymer separation is not required prior to CRM of PDXL from mixed waste streams.

We have developed an RD-CROP method that affords molecular weight control and living chain-end retention for the polymerization of cyclic acetal monomers. RD-CROP enables the synthesis of high molecular weight PDXL—a thermally stable, semicrystalline thermoplastic with high tensile strength suitable for large-scale applications such as packaging products. Moving forward, we are focusing on several major goals to improve upon the properties of PDXL and other CRM-enabled polyacetals. To begin, we are investigating new monomer designs to afford polyacetals that maintain moderate ceiling temperatures but show improved hydrophobicity and higher melting points that better mimic the properties of current commodity polymers. Next, we are optimizing the polymerization conditions to further meet the criteria of green chemistry, including bulk polymerization, using new initiating and quenching agents, and modifying the reaction workup. Lastly, we will explore stabilizers to afford improved oxidative and chemical stability of PDXL. Overall, we believe polyacetal synthesis via RD-CROP of cyclic acetals will prove an important strategy in the development of the circular plastics economy.

## REFERENCES AND NOTES

- R. Geyer, J. R. Jambeck, K. L. Law, *Sci. Adv.* **3**, e1700782 (2017).
- Z. O. G. Schyns, M. P. Shaver, *Macromol. Rapid Commun.* **42**, 2000415 (2021).
- J. M. Garcia, M. L. Robertson, *Science* **358**, 870–872 (2017).
- J. Brahney, M. Hallerud, E. Heim, M. Hahnenberger, S. Sukumaran, *Science* **368**, 1257–1260 (2020).
- E. MacArthur, *Science* **358**, 843–843 (2017).
- S. B. Borrelle *et al.*, *Science* **369**, 1515–1518 (2020).
- K. L. Law *et al.*, *Sci. Adv.* **6**, eabd0288 (2020).
- D. J. Fortman *et al.*, *ACS Sustain. Chem. Eng.* **6**, 11145–11159 (2018).
- S. Billiet, S. R. Trenor, *ACS Macro Lett.* **9**, 1376–1390 (2020).
- “Chemical Upcycling of Polymers,” Report of the Basic Energy Sciences Roundtable on Chemical Upcycling of Polymers, Bethesda, Maryland, 30 April to 1 May 2019; [https://science.osti.gov/-/media/bes/pdf/reports/2020/Chemical\\_Upcycling\\_Polymers.pdf](https://science.osti.gov/-/media/bes/pdf/reports/2020/Chemical_Upcycling_Polymers.pdf).
- Ellen MacArthur Foundation, “Universal circular economy policy goals” (2021); <https://policy.ellenmacarthurfoundation.org/universal-policy-goals>.
- J. C. Worch, A. P. Dove, *ACS Macro Lett.* **9**, 1494–1506 (2020).

13. A. Rahimi, J. M. García, *Nat. Rev. Chem.* **1**, 0046 (2017).
14. A. Kumar et al., *J. Am. Chem. Soc.* **142**, 14267–14275 (2020).
15. F. Zhang et al., *Science* **370**, 437–441 (2020).
16. C. Jehanno, M. M. Pérez-Madrigal, J. Demarteau, H. Sardon, A. P. Dove, *Polym. Chem.* **10**, 172–186 (2019).
17. D. E. Fagnani et al., *ACS Macro Lett.* **10**, 41–53 (2020).
18. W. W. Y. Lau et al., *Science* **369**, 1455–1461 (2020).
19. H. Höcker, *J. Macromol. Sci. Part A* **30**, 595–601 (1993).
20. H. Nishida et al., *Macromolecules* **44**, 12–13 (2011).
21. G. W. Fahrhorst, T. R. Hoye, *ACS Macro Lett.* **7**, 143–147 (2018).
22. L. Cederholm, P. Olsén, M. Hakkarainen, K. Odelius, *Polym. Chem.* **11**, 4883–4894 (2020).
23. J.-B. Zhu, E. M. Watson, J. Tang, E. Y.-X. Chen, *Science* **360**, 398–403 (2018).
24. X. Tang, E. Y.-X. Chen, *Chem* **5**, 284–312 (2019).
25. R. M. Cywar, J.-B. Zhu, E. Y.-X. Chen, *Polym. Chem.* **10**, 3097–3106 (2019).
26. Y. Liu, H. Zhou, J.-Z. Guo, W.-M. Ren, X.-B. Lu, *Angew. Chem. Int. Ed.* **56**, 4862–4866 (2017).
27. W. C. Ellis et al., *Chem. Sci.* **5**, 4004–4011 (2014).
28. D. J. Saxon, E. A. Gormong, V. M. Shah, T. M. Reineke, *ACS Macro Lett.* **10**, 98–103 (2021).
29. G. W. Coates, Y. D. Y. L. Getzler, *Nat. Rev. Mater.* **5**, 501–516 (2020).
30. J. P. Lutz et al., *J. Am. Chem. Soc.* **141**, 14544–14548 (2019).
31. S. Enthaler, *J. Appl. Polym. Sci.* **131**, 39791 (2014).
32. Y. Liu, Y. Jia, Q. Wu, J. S. Moore, *J. Am. Chem. Soc.* **141**, 17075–17080 (2019).
33. P. R. Christensen, A. M. Scheuermann, K. E. Loeffler, B. A. Helms, *Nat. Chem.* **11**, 442–448 (2019).
34. A. Hufendiek, S. Lingier, F. E. Du Prez, *Polym. Chem.* **10**, 9–33 (2018).
35. C. Shi et al., *Sci. Adv.* **6**, eabc0495 (2020).
36. M. Häußler, M. Eck, D. Rothauer, S. Mecking, *Nature* **590**, 423–427 (2021).
37. M. Hong, E. Y.-X. Chen, *Green Chem.* **19**, 3692–3706 (2017).
38. C. Suemitsu, A. Kanazawa, S. Aoshima, *Polym. Chem.* **12**, 822–830 (2021).
39. R. L. Snyder et al., *ACS Energy Lett.* **6**, 1886–1891 (2021).
40. M. A. Hillmyer, *Science* **358**, 868–870 (2017).
41. W. F. Gresham, Preparation of Polydioxolane, US Patent 2394910 (1946).
42. H. Qiu, Z. Yang, M. Köhler, J. Ling, F. H. Schacher, *Macromolecules* **52**, 3359–3366 (2019).
43. T. Higashimura, O. Kishiro, *Polym. J.* **9**, 87–93 (1977).
44. M. Sawamoto, J. Fujimori, T. Higashimura, *Macromolecules* **20**, 916–920 (1987).
45. R. Faust, J. P. Kennedy, *J. Polym. Sci. A Polym. Chem.* **25**, 1847–1869 (1987).
46. K. Maruyama, A. Kanazawa, S. Aoshima, *Polym. Chem.* **10**, 5304–5314 (2019).
47. R. Szymanski, P. Kubisa, S. Penczek, *Macromolecules* **16**, 1000–1008 (1983).
48. Y. C. Bae, R. Faust, *Macromol. Symp.* **132**, 11–23 (1998).
49. K. M. Osten, P. Mehrkhodavandi, *Acc. Chem. Res.* **50**, 2861–2869 (2017).
50. L. C. Reibel, C. P. Durand, E. Franta, *Can. J. Chem.* **63**, 264–269 (1984).
51. J. Fejgin, W. Sadowska, M. Tomaszewicz, S. Penczek, *Makromol. Chem.* **95**, 155–167 (1966).
52. J. Brandup, E. H. Immergut, E. A. Grulke, *Polymer Handbook* (Wiley, ed. 4, 2003).
53. P. H. Plesch, P. H. Westermann, *J. Polym. Sci. Part C Polym. Symp.* **16**, 3837–3843 (1967).
54. P. G. M. Wuts, T. W. Greene, *Greene's Protective Groups in Organic Synthesis* (Wiley-Interscience, ed. 4, 2007).

#### ACKNOWLEDGMENTS

The authors thank Y. D. Y. L. Getzler for invaluable discussion.

**Funding:** This work was fully supported by the Joint Center for Energy Storage Research (JCESR), an Energy Innovation Hub funded by the US Department of Energy, Office of Science, Basic Energy Sciences. This work made use of the Cornell Center for Materials Research and the NMR Facility at Cornell University, which are supported by the NSF under awards DMR-1719875 and CHE-1531632, respectively. **Author contributions:** B.A.A. and R.L.S. designed and performed all experiments. G.W.C. directed research. All authors prepared the manuscript. **Competing interests:** B.A.A., R.L.S., and G.W.C. are inventors on US provisional patent application D-9743, submitted by Cornell University, which covers synthesis of polyacetals by RD-CROP and their chemical recycling. **Data and materials availability:** All data are available in the manuscript or the supplementary materials.

#### SUPPLEMENTARY MATERIALS

science.sciencemag.org/content/373/6556/783/suppl/DC1  
Materials and Methods  
Synthetic Procedures  
Figs. S1 to S63  
Tables S1 to S29  
References (55–59)

12 February 2021; resubmitted 10 May 2021

Accepted 2 July 2021

10.1126/science.abh0626



## Chemically recyclable thermoplastics from reversible-deactivation polymerization of cyclic acetals

Brooks A. Abel Rachel L. Snyder Geoffrey W. Coates

*Science*, 373 (6556), • DOI: 10.1126/science.abh0626

### Tough recyclable polyacetals

Cyclic acetals such as dioxolane are appealing building blocks for recyclable plastics but have proven to be difficult to polymerize controllably. Abel *et al.* show that optimal pairing of a bromomethyl ether and indium or zinc Lewis acid produces polydioxolane with high tensile strength that may be advantageous for packaging applications. Heating this plastic in strong acid easily breaks it back down to its acetal monomer, which can then be recovered by distillation from mixed plastic waste streams in high yield. —JSY

### View the article online

<https://www.science.org/doi/10.1126/science.abh0626>

### Permissions

<https://www.science.org/help/reprints-and-permissions>

Use of this article is subject to the [Terms of service](#)

*Science* (ISSN ) is published by the American Association for the Advancement of Science. 1200 New York Avenue NW, Washington, DC 20005. The title *Science* is a registered trademark of AAAS.

Copyright © 2021 The Authors, some rights reserved; exclusive licensee American Association for the Advancement of Science. No claim to original U.S. Government Works